Photoisomerization of all-*trans*-1,6-Diphenyl-1,3,5-hexatriene. Temperature and Deuterium Isotope Effects†

Jack Saltiel,* Govindarajan Krishnamoorthy, Zhennian Huang, Dong-Hoon Ko, and Shujun Wang

Department of Chemistry and Biochemistry, Florida State University, Tallahassee, Florida 32306-4390

Received: July 1, 2002; In Final Form: October 19, 2002

Irradiation of all-*trans*-1,6-diphenyl-1,3,5-hexatriene (*ttt*-DPH) in acetonitrile (AN) gives *ctt*- and *tct*-DPH by relatively inefficient pathways but mainly via the singlet excited state. Assuming that twisted singlet excited state intermediates partition equally to cis and trans ground state double bonds leads to the conclusion that the major nonradiative decay process of the singlet excited state of *ttt*-DPH (^{1}*ttt*-DPH*) is direct decay to the *ttt*-DPH ground state, $\phi_{nr} = 0.54$. If CH stretching vibrations serve as accepting modes in this decay process, deuterium substitution should profoundly attenuate it. We report a comparative study of perhydro-*ttt*-DPH with di- and tetradeuterated *ttt*-DPH (*ttt*-DPH-d_n, $n = 0$, 2, and 4) involving deuteration of one and both terminal triene double bonds. NMR and HPLC analyses give $k_H/k_D = 1.36 \pm 0.1$ for terminal bond isomerization at 20.0 °C. The very small changes in τ_f and ϕ_f are consistent with such a kinetic deuterium isotope effect on the rate constant for terminal bond isomerization. The temperature dependencies of τ_f, ϕ_{ctt}, and ϕ_{tct} for ^{1}*ttt*-DPH-d_0* give energy barriers for torsional relaxations that are well above the $2A_g-1B_u$ energy gap. The major radiationless decay process is not related to trans → cis photoisomerization, is barrierless within experimental uncertainty, is completely insensitive to deuterium substitution, and occurs in the ns time scale. The mechanistic implications of these results are discussed.

Introduction

Our interest in all-*trans*-1,6-diphenyl-1,3,5-hexatriene (*ttt*-DPH) stems from its use as a model for long polyenes because it is the first member of the α,ω-diphenylpolyene vinylogous family whose lowest excited state is the forbidden doubly excited $2A_g$ state.[1−3] This state couples vibronically[4] with its precursor state, the initially formed $1B_u$ state, and the two mixed states exist in rapidly established[5,6,7] thermal equilibrium.[8] A crucial role for the $2A_g$ state in the photoisomerization of the stilbenes was proposed by Orlandi and Siebrand[9] (OS) and adopted in a generalized mechanism for the higher members of the α,ω-diphenylpolyene family by Birks.[10] A key assumption in the Birks mechanism, that in *ttt*-DPH, as in the stilbenes, torsional motion leading to photoisomerization is the only radiationless decay channel competing with fluorescence has been shown to be inconsistent with photoisomerization quantum yields measured in our laboratory.[11,12] Torsional barrier heights, estimated by Birks[10] from the temperature dependencies of fluorescence quantum yields and lifetimes,[13] on the basis of this assumption, are unreliable. Specifically, in degassed acetonitrile (AN) solutions, fluorescence, intersystem crossing, and photoisomerization account for only 34−44% of ^{1}*ttt*-DPH* decay at 20 °C,[12] depending on which ϕ_f literature value 0.16[13] or 0.26[14] is employed. It follows that, absent a very unfavorable branching ratio, the Birks analysis neglects a radiationless decay channel that in AN accounts for more than half of ^{1}*ttt*-DPH* deactivation without contributing to photoisomerization.

The energetics for the torsional relaxations about the terminal and central double bonds of ^{1}*ttt*-DPH* in AN are derived here from the dependencies of photoisomerization quantum yields and fluorescence lifetimes on temperature. In addition, we report the synthesis and comparative study of derivatives of *ttt*-DPH (*ttt*-DPH-d_n, $n = 2$ and 4) involving deuteration of one and both terminal triene double bonds. Surprisingly, in contrast to the photoisomerization decay channels, the major radiationless decay pathway of *ttt*-DPH is insensitive to *d*-substitution and to temperature.

Experimental Section

Materials. Sources and purification procedures for all-*trans*-1,6-diphenyl-1,3,5-hexatriene (100.0%, HPLC), benzophenone, *trans*-stilbene, anthracene, and acetonitrile were as previously described.[15] Reagents used in the syntheses were the best available commercially and, unless noted otherwise, were used as received. The syntheses of *ttt*-DPH-d_2 (99.9%, HPLC) and $-d_4$ (98.0%, HPLC, 1.7% *tcc*-DPH-d_4, major contaminant) were accomplished by deuteration of the corresponding acetylenes over Lindlar catalyst, followed by diphenyl diselenide catalyzed isomerization to predominantly all-trans equilibrium mixtures and purification. Synthetic details follow.

ttt-DPH-d_2: Triphenylcinnamylphosphonium Bromide. Cinnamyl bromide (1.97 g, 0.011 mol) and triphenyl phosphine (3.15 g, 0.012 mol) were dissolved in 20 mL of anhydrous benzene and stirred at room temperature for 24 h in a 100 mL round-bottom flask. Precipitated triphenylcinnamylphosphonium bromide was filtered, washed with ether to remove unreacted triphenyl phosphine, and dried over P_2O_5.

trans,trans- and trans,cis-1,6-Diphenyl-1,3-dien-5-yne. Butyllithium (3 mmol, 2.5 mol in hexane) was added dropwise by syringe over a 2 h period to a solution of triphenylcinnamylphosphonium bromide (1.38 g, 3 mmol) in 70 mL of

† Part of the special issue "George S. Hammond & Michael Kasha Festschrift". J.S. dedicates this paper to his inspiring teacher George S. Hammond with gratitude.

* To whom correspondence should be addressed.

10.1021/jp021540g CCC: $25.00
Published on Web 12/17/2002

anhydrous diethyl ether. The solution gradually became pink in color with the simultaneous precipitation of white lithium bromide. After stirring the mixture for 1 h at room temperature, an equimolar amount of phenylpropynal in anhydrous ether was added dropwise by syringe over a 1.5 h period. Stirring was continued until starting materials were depleted (TLC). Precipitated triphenylphosphine oxide was removed by filtration, and the filtrate was neutralized with acetic acid, washed with water, and dried over sodium sulfate. A yellow oil was obtained upon evaporation of diethyl ether. Addition of 20 mL of methanol led to precipitation of pure *trans,trans*-1,6-diphenyl-1,3-dien-5-yne as a light yellow solid (^{1}H NMR,[16] UV). Pure *trans,cis*-1,6-diphenyl-1,3-dien-5-yne was obtained from the filtrate by chromatography on silica gel with hexane as eluent (^{1}H NMR,[16] UV).

all-trans-1,6-Diphenyl-1,2-dideuterio-1,3,5-hexatriene (ttt-DPH-d_2). A mixture of *trans,trans*- and *trans,cis*-1,6-diphenyl-1,3-dien-5-yne (1.6 g, 7 mmol) was dissolved in 60 mL of anhydrous hexane (refluxed over sodium) containing Lindlar catalyst (10% w/w). A syringe attached to a balloon filled with deuterium gas was inserted into the reaction flask through a rubber stopper, and the progress of the reaction was monitored by GLC. Upon depletion of the starting materials, the catalyst was removed by filtration, and the filtrate was reduced to half its original volume under vacuum. Diphenyl diselenide (0.08 g, 5% w/w) was added, and the mixture was equilibrated by refluxing in room light for 1 h.[17] The *ttt*-DPH-d_2 was crystallized from the reaction mixture and isolated by filtration, 0.8 g, 50%. *ttt*-DPH-d_2: mp 198−199 °C; ^{1}H NMR (300 MHz, $CDCl_3$) δ 7.20−7.45 (10H, 2 Ph), 6.86−6.92 (1H), 6.58−6.62 (d, J = 16, 1H), 6.51−6.54 (2H); MS *m*/*z* 234 (M^+, 100%), 232 ($M^+ - 2$, 2.07%).

all-trans-1,6-Diphenyl-1,2,5,6-tetradeuterio-1,3,5-hexatriene (ttt-DPH-d_4). A mixture of *cis*- (major component) and *trans*-1,6-diphenyl-3-hexen-1,5-diynes was synthesized from *cis*-1,2-dichloroethene following the procedure described by Vollhardt and Winn.[18] Reduction of the 1,6-diphenyl-3-hexen-1,5-diynes (1.3 g, 5.7 mmol) with deuterium gas over Lindlar catalyst afforded a mixture of *ttt*- and *tct*-DPH-d_4 which was equilibrated with diphenyl diselenide as the radical source[17] (see above). The pure *ttt*-DPH-d_4 (0.7 g) was isolated in 53% yield: mp 198−199 °C; ^{1}H NMR (300 MHz, $CDCl_3$) δ 7.0−7.25 (tt, 2H, Ph), 7.30−7.35 (t, 4H, Ph), 7.41−7.44 (d, 4H, Ph), 6.52_4 (s, 2H); MS *m*/*z* 236 (M^+, 100%), 232 ($M^+ - 4$, 1.10%).

Irradiation Procedure. Irradiations were carried out in a Moses merry-go-round[19] apparatus immersed in a thermostated water bath. A heating coil connected to a thermoregulator (Polyscience corporation) was used to control the temperature to ±0.1 °C. The benzophenone-sensitized photoisomerization of *trans*-stilbene was used for actinometry, $\phi_{t\rightarrow c} = 0.55$.[20,21] A Hanovia medium-pressure Hg lamp (200 W, Ace Glass, Inc.) and Corning CS 7-37 and 0-52 filters were used for excitation at 366 nm. Solutions, 3.0 mL, were pipetted into Pyrex ampules, 13 mm o.d., degassed, and flame-sealed at a constriction. Sample preparation, degassing, and analysis were performed under nearly complete darkness (red light).

Analytical Procedures. Actinometer solutions were analyzed by GLC and DPH solutions by HPLC (λ_{mon} = 350 nm) as previously described,[12,15] except that, on replacing AN with hexanes prior to HPLC analyses, a stream of argon was used to evaporate the solvent and care was exercised to avoid taking samples to dryness. The ctt/ttc ratio from the terminal bond photoisomerization of *ttt*-DPH-d_2 in AN was determined from the ^{1}H NMR spectrum (500 MHz, acetone-d_6) of the isolated photoproduct. A Nova 500 MHz NMR spectrometer was employed. An analytic sample of *ctt*-DPH-d_0 was obtained by semipreparative HPLC of the mixture resulting on 366 nm excitation of an air-saturated AN solution of *ttt*-DPH-d_0 (1.0×10^{-3} M).[22] ^{1}H NMR peak assignments were based unambiguously on a Phase Sensitive COSY spectrum: (500 MHz, acetone-d_6) δ 6.37−6.42 (dd, $J_{b'a'}$ = 12.0 Hz, $J_{b'c'}$ = 12.0 Hz, $H_{b'}$), 6.47−6.51 (d, $J_{a'b'}$ = 12.0 Hz, $H_{a'}$), 6.62−6.67 (dd, $J_{cc'}$=15.0 Hz, J_{cb}=12.0 Hz, H_c), 6.68−6.72 (d, J_{ab} = 15.5 Hz, H_a), 6.98−7.04 (dd, $J_{c'c}$ = 15.0 Hz, $J_{c'b'}$ = 12.0 Hz, $H_{c'}$), 7.04−7.09 (dd, J_{ba}= 15.5 Hz, J_{bc} = 12.0 Hz, H_b), 7.21−7.27 (m, 1H), 7.27−7.30 (m, 1H), 7.31−7.36 (m, 2H), 7.37−7.43 (m, 4H), 7.49−7.51 (m, 2H).

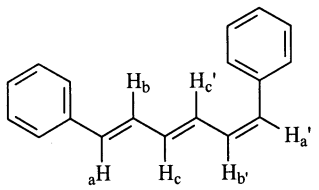

ttc-DPH-d_0

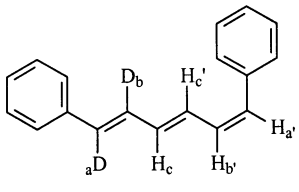

ttc-DPH-d_2

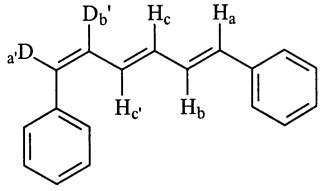

ctt-DPH-d_2

Ar bubbled *ttt*-DPH-d_2, 1.0×10^{-3} M in AN, was irradiated at 366 nm in a Hanovia reactor. The irradiation was stopped at 20% over all conversion (13.5% ctt, 6.8% tct). AN was removed completely under reduced pressure. The products were separated partially by column chromatography on activity I alumina with 30% *n*-pentane in benzene (v/v) as eluent and fractions rich in *ctt*/*ttc*-DPH-d_2 were subjected to semipreparative HPLC separation to yield pure *ctt*/*ttc*-DPH-d_2 for ^{1}H NMR analysis: (500 MHz, acetone-d_6) δ 6.37−6.42 (dd, $J_{b'a'}$ = 12.0 Hz, $J_{b'c'}$ = 12.0 Hz, $H_{b'}$, ttc), 6.47−6.51 (d, $J_{a'b'}$ = 12.0 Hz, $H_{a'}$, ttc), 6.62−6.67 (m, H_c, ttc, H_c, ctt), 6.68−6.72 (d, J_{ab} = 15.5 Hz, $H_{a'}$, ctt), 6.98−7.04 (m, $H_{c'}$, ttc, $H_{c'}$, ctt), 7.04−7.09 (m, H_b, ctt), 7.21−7.27 (m, 1H), 7.27−7.30 (m, 1H), 7.31−7.36 (m, 2H), 7.37−7.43 (m, 4H), 7.49−7.51 (m, 2H). The spectrum is shown in Figure 1.

Fluorescence Measurements. Fluorescence spectra were measured with a Hitachi F-4500 spectrophotometer equipped with a 150-W Xe arc source and a Hamamatsu R3788 photomultiplier tube. The scan rate was 2400 nm/min and slit widths were set at 2.5 nm for both excitation and emission monochromators. (The Hitachi F-4500 employs horizontal excitation and emission slits, instead of vertical.) Fluorescence spectra were recorded for both air saturated and Ar bubbled solutions of DPH in acetonitrile in standard 1 cm^2 quartz cells. Temperature was maintained at 20.0 ± 0.1 °C using a Neslab-RTE 4DD constant temperature circulation bath and was monitored continuously during each scan with an Omega Engineering model 199 RTD digital thermometer in a reference cell placed in the same constant temperature cell holder. Absorption spectra were recorded with a Cary 300 UV−Vis spectrophotometer at 20.0 °C. Fluorescence quantum yields were determined using quinine sulfate in 1 N H_2SO_4 ($\phi_f = 0.54_6$ at 25.0 °C, adjusted to 0.55_3 for 20.0 °C)[21,22] as reference standard. Absorbances of samples and reference, A_s and A_r, respectively,

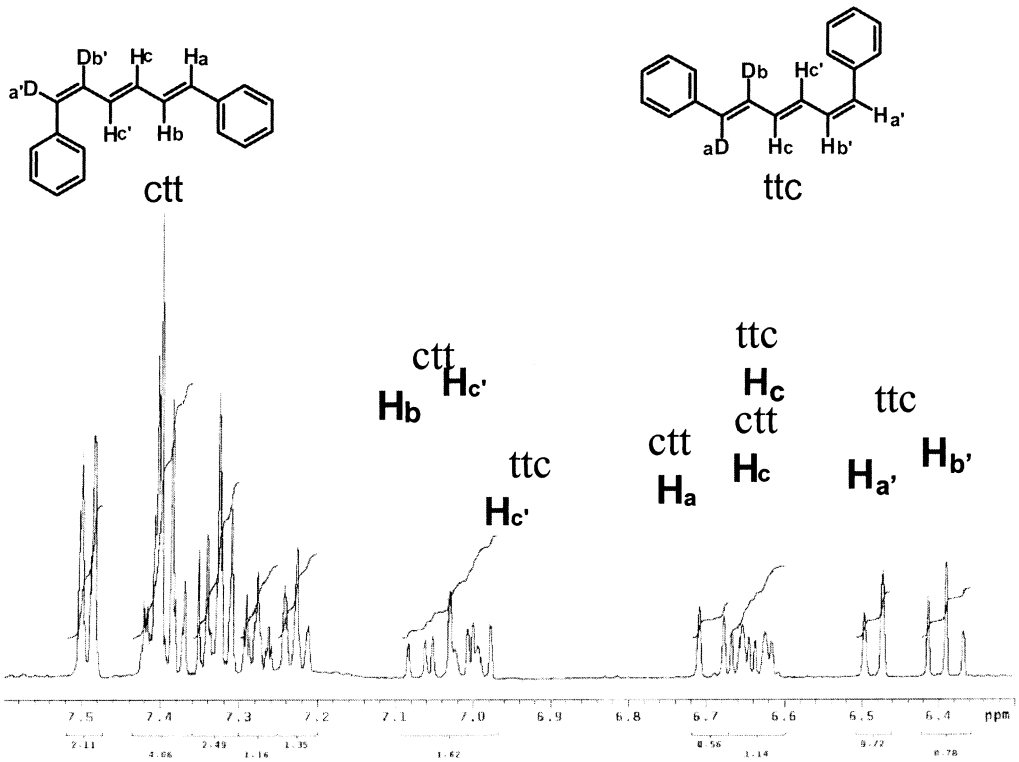

Figure 1. ^{1}H NMR of the *ttc*- and *ctt*-DPH-d_2 mixture obtained on 366 nm irradiation of *ttt*-DPH-d_2, see text.

were matched at ~0.1 at $\lambda_{exc} = 365$ nm. Corrections for differences in solvent refractive index, n, and absorbance at λ_{exc} were applied using

$$\phi_f^s = \phi_f^r (A_s A_r n_s^2)/(A_r A_s n_r^2) \quad (1)$$

where the fluorescence areas A_s and A_r of the sample and the reference, respectively, are corrected for nonlinearity in instrumental response. Fluorescence lifetimes were measured with a phase modulation Fluorolog-τ2 lifetime spectrofluorometer (SPEX) equipped with a 450-W Xe arc source, a Hamamatsu R928P photomultiplier tube, and a Lasermetrics BNC1072FW Pockel cell (KD_2PO_4). The Fluorolog-τ2 modulates the frequency of the excitation light from 0.5 to 300 MHz. A glycogen solution ($\tau = 0$ ns, scattered light) was used as reference. Temperatures were maintained and measured as described above. DPH solutions (2.0×10^{-6} M) were degassed using 8 freeze−pump−thaw cycles to 4×10^{-6} Torr and flame-sealed at a constriction. A 13 mm o.d. tube attached to a standard 1 cm^2 quartz cell via a sidearm and a graded seal was employed. Software (DMF 3000F Spectroscopy) provided by the manufacturer was used to analyze the data. Determinations of the quality of the lifetimes were based on examination of the statistics of a fit (a plot of the residual deviations vs frequency) and reduced χ^2 values that were all close to unity.

Results

Photochemical Observations. Photostationary states were approached from *ttt*-DPH-d_n ($n = 2$ and 4). Degassed DPH samples (1.0×10^{-3} M) in AN were irradiated for different time intervals at 20.0 °C until HPLC analysis revealed no further change in the isomer composition. Photostationary state fractions are shown in Table 1 together with corresponding values determined earlier[10] for *ttt*-DPH-d_0. Overall conversions for quantum yield measurements were kept below 2.5% and were corrected for back reaction as previously described.[12] They are also shown in Table 1. A value of 1.35 was calculated from the ^{1}H NMR spectrum in Figure 1 for the ttc/ctt ratio of the terminal bond isomerization products from the irradiation of *ttt*-DPH-d_2 using the ratio of the average integrations of the signals at δ 6.37−6.42 ($H_{b'}$, ttc) and 6.47−6.51 ($H_{a'}$, ttc) to the area of the signal at δ 6.68−6.72 (H_a, ctt). The dependence of photoisomerization quantum yields on temperature was measured starting from *ttt*-DPH-d_0 and the results are shown in Table 2.

TABLE 1: PSS Fractions and Photoisomerization Quantum Yields for *ttt*-DPH-d_n in Degassed AN (366 nm, 20.0 °C)

PSS Fractions				
compound	ttc + ctt	tct	tcc + cct	ttt
ttt-DPH-d_0[a]	0.239	0.106	0.020	0.635
ttt-DPH-d_2	0.206	0.106	0.027	0.667
ttt-DPH-d_4	0.183	0.115	0.025	0.661

Quantum Yields				
compound	ϕ_{ctt}	ϕ_{tct}	ϕ_{cct}[c]	k_H/k_D
ttt-DPH-d_0	0.062	0.035	0.005_1	
ttt-DPH-d_2	0.054	0.036	0.007_3	1.35[b]
ttt-DPH-d_4	0.046	0.038	0.005_6	1.37

[a] From ref 12. [b] From the quantum yields and by ^{1}H NMR. [c] No back reaction correction was applied to this two-photon process.

Fluorescence Measurements. Absorption and fluorescence spectra of the set of *ttt*-DPH$_n$ in AN at 20 °C are shown in Figure 2. Fluorescence quantum yields, measured for Ar- and air-saturated AN solutions, and fluorescence lifetimes measured for degassed and air-saturated solutions at 20.0 °C are shown in Table 3. Fluorescence quantum yields for Ar-saturated solutions and fluorescence lifetimes for degassed solutions at different temperatures are included in Table 2. Excellent fits to the single-exponential decay model were obtained ($\chi^2 \leq 1.2$), and the lifetimes were independent of excitation and monitoring wavelengths, within experimental uncertainty. Reproducibility in independent measurements was better than ±0.1 ns.

Discussion

The separation into singlet and triplet components of the photoisomerization quantum yields of *ttt*-DPH-d_0 in degassed AN upon 366 nm has been based on the following mechanism[12]

$$^1\text{ttt} \xrightarrow{h\nu} {}^1\text{ttt}^* \quad (2)$$

$$^1\text{ttt}^* \xrightarrow{k_f} {}^1\text{ttt} + h\nu \quad (3)$$

$$^1\text{ttt}^* \xrightarrow{k_{nr}} {}^1\text{ttt} \quad (4)$$

$$^1\text{ttt}^* \xrightarrow{k_{is}} {}^3\text{eet}^* \quad (5)$$

$$^1\text{ttt}^* \xrightarrow{k_1} {}^1\text{ptt}^* \quad (6)$$

$$^1\text{ttt}^* \xrightarrow{k_3} {}^1\text{tpt}^* \quad (7)$$

$$^1\text{ptt}^* \xrightarrow{k_{dl}} \alpha'{}^1\text{ctt} + (1-\alpha'){}^1\text{ttt} \quad (8)$$

$$^1\text{tpt}^* \xrightarrow{k_{d2}} \beta'{}^1\text{tct} + (1-\beta'){}^1\text{ttt} \quad (9)$$

$$^3\text{eet}^* \xrightarrow{k_d} \alpha{}^1\text{ctt} + \beta{}^1\text{tct} + (1-\alpha-\beta){}^1\text{ttt} \quad (10)$$

$$^3\text{eet}^* + {}^1\text{ttt} \xrightarrow{k_{ttt}} \gamma{}^1\text{ctt} + \delta{}^1\text{tct} + (\gamma_{en}+\delta_{en}){}^3\text{eet}^* + [2(1-\gamma-\delta)+\gamma_q+\delta_q]{}^1\text{ttt} \quad (11)$$

where "p" designates a twisted double bond (e.g., ptt indicates twisting at a terminal double bond), "e" designates a double bond that exists as an equilibrium mixture of planar geometries,[17] and the greek letters are decay fractions from twisted singlets and from equilibrated planar triplets. Application of the steady-state approximation to all excited species gives quantum yield expressions 12 and 13 for *ctt*-DPH and *tct*-DPH formation:

$$\phi_{ctt} = \alpha' k_1 \tau_s^o + \frac{\phi_{is}^o(\alpha + \gamma\, k_{ttt}\, \tau_T^o[^1\text{ttt}])}{1 + (1-\gamma_{en}-\delta_{en})k_{ttt}\, \tau_T^o[^1\text{ttt}]} \quad (12)$$

$$\phi_{tct} = \beta' k_3 \tau_S^o + \frac{\phi_{is}^o(\beta + \delta\, k_{ttt}\, \tau_T^o\, [^1\text{ttt}])}{1 + (1-\gamma_{en}-\delta_{en})\, k_{ttt}\, \tau_T^o[^1\text{ttt}]} \quad (13)$$

where $\tau_S^o = (k_f + k_{nr} + k_{is} + k_1 + k_3)^{-1}$ is the singlet lifetime of *ttt*-DPH and $\tau_T^o = k_d^{-1}$ is the lifetime of the equilibrated triplet. The first terms on the right-hand side of the equal signs in eqs 12 and 13 are the singlet contributions, ϕ_{xxt}^S, and the second terms are the triplet contributions, ϕ_{xxt}^T, to the observed quantum yields. The very low intersystem crossing yield in AN, $\phi_{is}^0 = 0.01$,[12] and the previously defined parameters for DPH triplets have led to the conclusion that, at 20.0 °C, photoisomerization in this solvent is due primarily to the singlet pathway.[12] This conclusion is consistent with the results in Table 1. The new ϕ_{tct} value agrees exactly with our previous value,[12] and the new ϕ_{ctt} value is 10% higher, probably because *ctt*-DPH survives better under the milder conditions used to replace the solvent prior to HPLC analysis. Nearly all terminal bond photoisomerization (98.3%) and most central bond isomerization (83.2%) occur in the singlet manifold.

Energetics of Torsional Relaxation in *ttt*-DPH-d_0. The temperature dependencies of photoisomerization quantum yields and fluorescence lifetimes in Table 2 can be used to estimate torsional barriers for twisting about the terminal and central double bonds of *ttt*-DPH-d_0, based on the above mechanism. Examination of Table 2 shows that our lifetime values are systematically higher than earlier values,[13] probably because of the difference between imperfect outgassing and our thorough degassing. We proceed, initially, by neglecting the ϕ_{xxt}^T contributions, because they are small and their temperature dependencies are not known in AN. Plots of $\ln(\phi_{xxt}/\tau_S^o)$ vs T^{-1}, Figure 3, are, to a very good approximation (excellent in the case of terminal bond isomerization), equivalent to Arrhenius plots of the quantities $\alpha' 2k_1$ (there are two equivalent terminal bonds) and $\beta' k_3$. Assuming, by analogy with stilbene,[25] temperature

TABLE 2: Temperature Effects on Photoisomerization and Fluorescence Quantum Yields of *ttt*-DPH-d_0 and of Fluorescence Lifetimes of *ttt*-DPH-d_n in Degassed AN (366 nm)

T, °C	$\phi_{ttt\rightarrow ttc}$	$\phi_{ttt\rightarrow tct}$	ϕ_f,[a]	τ_{d0},[a] ns	τ_{d2}, ns	τ_{d4}, ns
2.5	0.030_1	0.021_8				
10.0			0.30_8 (0.22)	5.3 (4.7, 5.1)	5.3	5.4
15.5	0.049_1	0.029_4				
17.2	0.051_1	0.032_4				
20.0	0.061_6	0.034_6	0.26_9 (0.16)	4.7 (3.9, 4.7)	4.8	4.8
30.0			0.23_3 (0.13)	4.1 (3.3, 4.3)	4.1	4.2
30.1	0.089_3	0.042_4				
35.0	0.087_9	0.055_2				
40.0			0.20_1 (0.10)	3.6 (2.8, 3.8)	3.6	3.8
44.4	0.131_0	0.056_2				
50.0			0.16_4 (0.085)	3.0 (2.4. 3.2)	3.2	3.4
57.5	0.179_5	0.074_7				
57.7	0.201_7	0.079_3				
60.0			0.15_2 (0.22)	2.8 (2.1, 2.7)	2.9	3.1

[a] The first values in parentheses are interpolated from ref 13; the second values in the lifetime column are calculated from the rate constants in Table 4 by assigning all T-dependence to the twisting rate constants in eqs 6 and 7, see text.

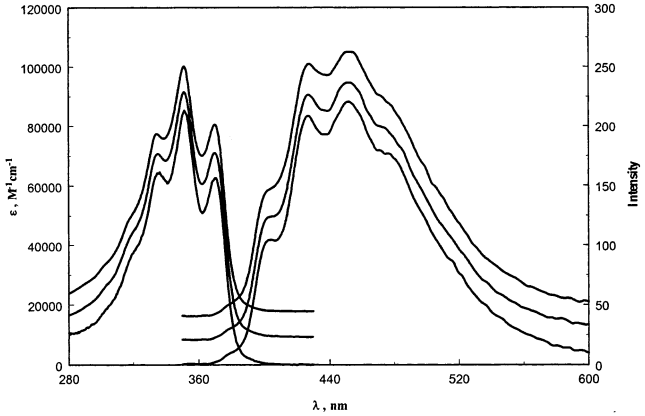

Figure 2. Absorption and fluorescence spectra of *ttt*-DPH-d_n (λ_{exc} = 365 nm, 20.0 °C). The $n = 2$ and 4 spectra are successively displaced on the ordinate scale to facilitate comparison.

TABLE 3: Fluorescence Quantum Yields and Lifetimes of *ttt*-DPH-d_n in AN, 20.0 °C

			τ, ns		
compound	ϕ_f	ϕ_f^{Ar}/ϕ_f^{Air}	degassed	air	τ_0/τ
ttt-DPH-d_0	0.26_9	1.29 (1.32)[a]	4.69	3.50	1.34
ttt-DPH-d_2	0.27_1	1.30	4.77	3.72	1.30
				3.61	
				3.64	
ttt-DPH-d_4	0.27_9	1.30	4.76	3.57	1.33
	0.27_7		4.76	3.60	1.32
			4.75	3.67	1.29

[a] The value in parentheses is for a degassed instead of an Ar-saturated solution; see also ref 12.

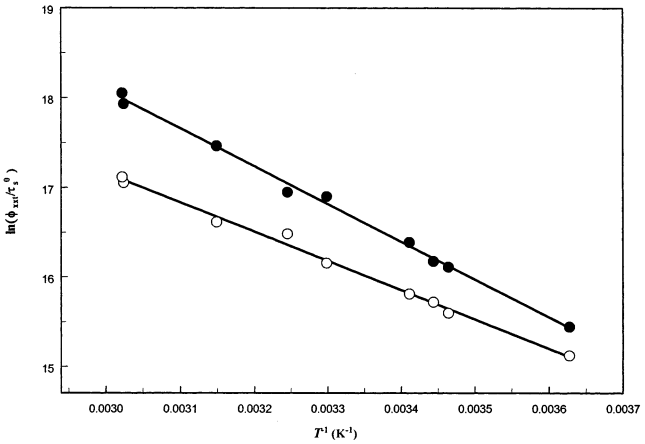

Figure 3. Temperature effect on twisting rate constants for terminal (closed circles) and central (open circles) bonds of ^{1}*ttt*-DPH-d_0*.

independent decay fractions from the twisted intermediates, the slopes of the lines in Figure 3 give $E_{ptt} = 8.40 \pm 0.20$ kcal/mol and $E_{tpt} = 6.52 \pm 0.20$ kcal/mol as the activation energies for torsional relaxation about the terminal and central double bonds in ^{1}*ttt*-DPH-d_0*. Both of these values place the torsional barriers well above the spectroscopically estimated $2^1A_g/1^1B_u$ energy

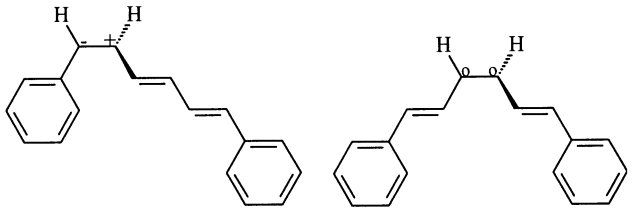

^{1}*ptt*-DPH* ^{1}*tpt*-DPH*

gap of 4.1 kcal/mol. Arrhenius *A* factors, can be estimated from the intercepts of the plots in Figure 3 (30.77 ± 0.34 and 27.02 ± 0.33 for terminal and central double bonds, respectively) by assuming $\alpha' \cong \beta' \cong 0.5$. The resulting values are $A_{ptt} = (2.30 \pm 0.91) \times 10^{13}$ and $A_{tpt} = (1.08 \pm 0.40) \times 10^{12}$ s^{-1}. We will show below that adjusting the isomerization quantum yields by subtracting approximated triplet contributions does not seriously affect these parameters. Similar temperature effects, observed on photoisomerization quantum yields in the hydrocarbon solvents benzene and methylcyclohexane (MCH), are not as easily interpreted because of much more significant triplet contributions that cannot be neglected.[26] However, one important conclusion is inescapable. The selective, more than 20-fold enhancement of terminal bond isomerization on increasing solvent polarity from MCH to AN is consistent with the proposed zwitterionic *ptt*-DPH twisted intermediate.[11,12] It is caused by a pronounced enhancement of the frequency factor. It is not consistent with the usual explanation of a lowering of the torsional barrier by the polar solvent.[3] If anything, the barrier for terminal bond twisting in ^{1}*ttt*-DPH-d_0* is higher in AN. Previous derivations of overall effective torsional barriers (3.4 kcal/mol[10] and 5.3 kcal/mol[13] in AN) based only on fluorescence measurements yielded significantly underestimated values because of the erroneous assumption that all radiationless decay is along photoisomerization coordinates.

Deuterium Isotope Effects. Triplet lifetime enhancement upon perdeuteration of aromatic hydrocarbons was important in the development of theories of radiationless transitions.[27−29] As the T_1-S_0 energy gap decreases, intersystem crossing rate constants increase and the kinetic deuterium isotope effect (DIE) becomes less pronounced.[30] Such effects were associated with differences in vibrational overlap Franck−Condon factors, that is, mainly the relative ability of CH and CD stretching vibrations in the ground state to function as accepting modes for the electronic energy.[27−29] Recognition that *d*-substitution effects on intersystem crossing rate constants depend also on the position of substitution[31−35] led to the proposal that specific out-of-plane CH (CD less well) vibrations enhance spin−orbit coupling between π and σ states.[36]

The comparative study of deuterated DPH derivatives was initiated in order to determine (a) how the dominant radiationless decay component, which is along coordinates that are unproductive with respect to trans → cis isomerization, responds to *d*-substitution and (b) whether DIEs on photophysical and photochemical processes in *ttt*-DPH are consistent with known, highly position-dependent deuterium isotope effects on the excited states of stilbene. Specifically, the lifetime of the perpendicular triplet state of stilbene, ^{3}p*, increases by 30% on deuteration of the ethylenic positions[37,38] but is not affected by perdeuteration of the aromatic positions.[37] Only in rigid media at low temperatures where the *trans*-stilbene triplet maintains a planar geometry is there a measurable increase in the triplet lifetime on deuterium substitution of the aromatic positions.[37,39] In solution, the deuterium isotope effect on the torsional relaxation of the singlet excited state of *trans*-stilbene, ^{1}t*, is also specific to substitution of the ethylenic hydrogens.[40,41] Simultaneous analysis of the temperature dependencies of τ_f and ϕ_f values has led to the conclusion that the torsional barrier is enhanced slightly in ^{1}t*−d_2 (0.2 and 0.3 kcal/mol in *n*-hexane and *n*-tetradecane, respectively).[41,42] At 20 °C in *n*-hexane, where most stilbene singlets decay along the ^{1}t* → ^{1}p* relaxation coordinate, the effect on the twisting rate constant is nearly identical to the effect on the fluorescence quantum yields, $k_H/k_D = 1.6$.[41] A factor of 2 attenuation of the radiationless decay rate constant was observed earlier for the isolated molecules under jet-cooled conditions on perdeuteration of *trans*-stilbene for excitation above the torsional barrier.[43] These DIEs are accounted for satisfactorily by RRKM calculations which, for the favored $1^1B_u \rightarrow 2^1A_g$ crossing mechanism, predict an activation energy increase of 0.28 kcal/mol on substitution of the two vinyl-Hs,[44] consistent with experiment.[41] The magnitude of this effect appears to be related to the torsional barrier height because (a) there is no DIE on ^{1}c* → ^{1}p*, the barrierless torsional relaxation of *cis*-stilbene in *n*-hexane,[45] and (b) *d*-substitution of the single vinyl H of *trans*-1-phenylcyclohexene gives $k_H/k_D = 2.0$ over a 12.1 kcal/mol trans → cis torsional barrier.[46] Theoretical calculations (ab initio MCSCF with 6−31 G* and/or 6−311 G** basis sets) indicate that the loss of zero-point energy, primarily responsible for large predicted kinetic DIEs in the thermal cis → trans isomerizations of alkenes, involves a number of vibrational modes instead of a single torsional mode.[47] These calculations were bolstered by the observation of $k_H/k_D = 1.5$ at 287 °C for the thermal cis → trans isomerization of *cis*-stilbene on *d*-substitution of its two vinyl-Hs.[47] Also relevant to our study are DIEs on the interconversion of the *cis*- and *trans*-2,5-di-*tert*-butyl-1,3,5-hexatienes.[48] The small photoisomerization quantum yields in diethyl ether, 0.046 and 0.052 in the trans → cis and cis → trans directions, respectively, are attenuated by about 40% on deuteration of the central CC bond, consistent with $k_H/k_D = 1.6$ in both directions. Strong involvement of out-of-plane CH vibrations in the path to photoisomerization was suggested.[49]

We consider first the DIE on the isomerization of the terminal bonds in ^{1}*ttt*-DPH*. Because the first term in eq 12 accounts

TABLE 4: Photophysical Parameters of *ttt*-DPH-d_n in AN, 20.0 °C

compound	$10^{-7}k_f$, s^{-1}	$10^{-7}k_{1H}$,[a] s^{-1}	$10^{-7}k_{1D}$,[a] s^{-1}	$10^{-7}k_3$,[b] s^{-1}	$10^{-7}k_{is}$,[c] s^{-1}	$10^{-7}k_{nr}$,[d] s^{-1}
ttt-DPH-d_0	5.7_4	$2.6_0/2$		1.2_4	0.2_1	11.5
ttt-DPH-d_2	5.6_8	1.2_8	0.9_4	1.2_6	0.2_1	11.6
ttt-DPH-d_4	5.8_4		$1.8_9/2$	1.3_4	0.2_1	11.7
Ave.	5.7_5	1.2_9	0.9_4	1.2_8	0.2_1	11.6

[a] Based on quantum yields in Table 1, adjusted for triplet component (0.001, see ref 12); these quantities represent $2k_{1H}$, $k_{1H} + k_{1D}$, and $2k_{1D}$ for *ttt*-DPH-d_0, *ttt*-DPH-d_2, and *ttt*-DPH-d_4, respectively. [b] Based on quantum yields in Table 1, adjusted for triplet component (0.006, see ref 12). [c] Based on $\phi_{is} = 0.01$ from ref 14. [d] The difference between τ_f^{-1} and $\sum k_i$, where the k_i are the entries in the preceding columns.

for more than 98% of ϕ_{ctt} at 20 °C,[12] the ratio k_{1H}/k_{1D} can be obtained from

$$k_{1H}/k_{1D} = (\alpha'_H/\alpha'_D)(\phi_{ctt}^{d0}/\phi_{ctt}^{d4})(\tau_{d4}/\tau_{d0}) \qquad (14)$$

by assuming that the decay fraction is not affected by *d*-substitution ($\alpha'_H = \alpha'_D$), as is the case for stilbene singlets and triplets.[49] Substitution of the ratios of the observed quantum yields (Table 1) and fluorescence lifetimes (Table 3) for *ttt*-DPH-d_0 and *ttt*-DPH-d_4 into eq 14 gives $k_{1H}/k_{1D} = 1.37$, in excellent agreement with 1.35, the value obtained by ^{1}H NMR analysis of the *ttc*- and *ctt*-DPH photoproduct ratio from *ttt*-DPH-d_2. The observation that ϕ_{ctt} for *ttt*-DPH-d_2 exactly equals the average of the corresponding quantum yields for *ttt*-DPH-d_0 and *ttt*-DPH-d_4 provides further confirmation of these independent inter- and intramolecular determinations of k_{1H}/k_{1D}. The effect is smaller than the corresponding value for the ^{1}t* → ^{1}p* process in *trans*-stilbene but is consistent[47] with the proposed torsional relaxation mechanism for terminal bond isomerization.[11,10]

Our fluorescence quantum yield for *ttt*-DPH-d_0 in AN at 20.0 °C, Table 2, is higher than the first reported value[13] but agrees with 0.26, the value reported by Schael and Löhmannsröben.[14] Our lifetimes are systematically higher than those reported by Cehelnik et al.,[13] Table 2, and the 4.1 ns value measured at 20.0 °C by Schael and Löhmannsröben.[14] The reproducibility of our values (to ±0.1 ns in independent experiments, Table 3) and the difference in deaerating procedures suggests that residual oxygen was responsible, at least in part, for the lower quantum yields and lifetimes reported earlier.

Except for a small loss in vibronic resolution in the fluorescence spectra, the spectra of *ttt*-DPH are nearly independent of *d*-substitution, Figure 2. Fluorescence quantum yields and lifetimes, Tables 2 and 3, reveal little enhancement on deuteration. Much bigger changes would apply if k_{nr}, the rate constant for the major decay process of ^{1}*ttt*-DPH*, eq 4, were affected. Effective radiative rate constants k_f (ϕ_f/τ_f ratios at 20.0 °C, Table 3) are nearly identical, Table 4. The average value, 5.75×10^7 s^{-1}, is assumed to apply to the three members of our *ttt*-DPH-d_n series. Rate constants for the other unimolecular decay processes, also derived from quantum yield-to-lifetime ratios, are collected in Table 4. Calculation of the torsional relaxation rate constants of the excited singlet state was based on the isomerization yields corrected for the ϕ_{xxt}^Ts, the triplet contributions. The latter, taken from ref 12, were assumed to be independent of *d*-substitution. Assignment of the unaccounted for portions of the decay rates results in k_{nr} values that are independent of *d*-substitution. Multiplied by the observed lifetimes, they give nearly identical ϕ_{nr} values of 0.54, 0.55, and 0.56 for *ttt*-DPH-d_0, *ttt*-DPH-d_2, and *ttt*-DPH-d_4, respectively, the increase reflecting the slight change in lifetime. As expected, the minor correction for photoisomerization in the triplet state does not affect significantly the rate constants for terminal bond twisting nor does it affect the DIE for that process, $k_{1H}/k_{1D} = 1.37$, Table 4. The decrease in the rate constant for terminal bond twisting, alone, accounts for the small changes in fluorescence quantum yields and lifetimes. Use of the average rate constants in Table 4 predicts (τ_f, ϕ_f) pairs of (4.67 ns, 0.268), (4.75 ns, 0.273), and (4.83 ns, 0.278) for *ttt*-DPH-d_0, *ttt*-DPH-d_2, and *ttt*-DPH-d_4, respectively. The agreement with the observed values, Table 3, is excellent.

Corrected Torsional Relaxation Energy Barriers. Because the temperature effect on τ_f for *ttt*-DPH-d_0, Table 2, is accounted for, almost exactly, if one assumes that the isomerization channels are the only temperature-dependent processes, we were encouraged to further refine the derivation of the Arrhenius parameters for twisting by calculating approximate net isomerization quantum yields along the singlet excited-state pathways. The known triplet contributions to the photoisomerizations at 20 °C were assumed to vary with temperature in the same way as the quantities $\phi_{is}\alpha$ and $\phi_{is}\beta$. The temperature dependence of the intersystem crossing quantum yield, ϕ_{is}, was obtained from the measured fluorescence lifetimes by assuming that k_{is} (Table 4) is *T*-independent and that the triplet decay fractions, α and β, have the same temperature dependencies in AN as they do in benzene.[17] Arrhenius plots (not shown) of torsional relaxation rate constants based on the estimated singlet pathway isomerization quantum yields give $E_{ptt} = 8.48 \pm 0.20$ kcal/mol and $E_{tpt} = 7.38 \pm 0.25$ kcal/mol as the activation energies for torsional relaxation about the terminal and central double bonds in ^{1}*ttt*-DPH-d_0*. The corresponding Arrhenius frequency factors are $A_{ptt} = (2.60 \pm 1.07) \times 10^{13}$ and $A_{tpt} = (3.84 \pm 2.0) \times 10^{12}$ s^{-1}. The activation parameters for terminal bond twisting are identical within experimental uncertainty to those derived above without this correction. Changes in the activation parameters for central bond twisting are more pronounced, but the overall conclusions are not affected.

Assuming that torsional relaxations along photoisomerization coordinates are the only *T*-dependent processes and using the refined Arrhenius parameters to calculate the rate constants improves the agreement between calculated and observed fluorescence lifetimes slightly, Table 2. Precisely stated, agreement between observed and calculated lifetimes is attained by assuming that the sum of the rate constants k_f, k_{nr}, and k_{is} is *T*-dependent. We conclude that if one of these rate constants actually varies with *T*, complementary changes in the other two must compensate for this variation. Furthermore, because k_{is} is negligibly small, the sum of $k_f + k_{nr}$ is insensitive to *T*.

Rate Constants for the Major Decay Paths. The *T*-dependence of the effective radiative rate constant k_f was obtained from the τ_f and ϕ_f values in Table 2. Normally, radiative rate constants for allowed transitions decrease slightly with increasing temperature because of their dependence on the index of refraction. For instance, for the allowed $1B_u \rightarrow 1A_g$ transition in *trans*-stilbene, k_f decreases by less than 4% for a temperature increase of 60 °C in *n*-alkane solvents.[41] In *ttt*-DPH, the situation is much more complex because (a) the major portion of the emission originates from the $2A_g$ state and is forbidden,[1,2] (b) there is competing fluorescence from the nearby $1B_u$ state (the two states, $1B_u$ and $2A_g$, are vibronically coupled and exist as an equilibrium mixture in the all-s-trans conformer of *ttt*-DPH),[8] (c) the degree of coupling and, therefore, the magnitudes of the radiative rate constants k_{fA} and k_{fB} depend on the $1B_u/2A_g$ energy gap, which in turn is *T*-dependent because the energy of the $1B_u$ state decreases with increasing

polarizability (decreasing T), and (d) fluorescence also stems from the s-cis,s-trans conformer and its contribution increases with increasing T (excitation at the red edge of the absorption spectrum leads to enhanced emission at longer wavelengths as has been reported for methylcyclohexane).[50] Our ϕ_f values are larger than earlier values,[13] Table 2. We consider our quantum yields more reliable because our value at 20 °C agrees with a subsequent determination[14] and because ref 13 also reports small τ_f values. Effective radiative rate constants (k_f) obtained from the ϕ_f/τ_f ratios increase from 5.42×10^7 at 60 °C to 5.81×10^7 s^{-1} at 10 °C. The 7% change is marginally larger than the change experienced by the radiative rate constant of *trans*-stilbene. It suggests that the small decrease in k_{fA} with increasing T (because of the increase in the $1B_u/1A_g$ energy gap) is nearly exactly canceled by expected increases that should accompany the larger fractions of fluorescence from the two higher energy components.

Complementary changes in the rate constant k_{nr} of the major radiationless decay process predict a very modest 3.4% increase over the 10−60 °C T range, corresponding to a negligible activation energy, E_{nr}, of 0.13 kcal/mol. This activation energy is much smaller than ΔE_{BA}, the $1^1B_u/2^1A_g$ energy gap, ensuring that the radiationless process in eq 4 originates in S_1. The rate constant for eq 4 is enhanced from 2.2×10^7 to 1.15×10^8 s^{-1} on changing the solvent from MCH to AN.[10] In both solvents, the radiationless transition is faster than $k_{nr} = 1.2 \times 10^6$ s^{-1}, the value expected from Siebrand's energy-gap law[51] for polynuclear aromatic hydrocarbons with the same S_1-S_0 energy gap as DPH. This process originates in the lowest excited singlet state and returns the system to the original ground state. It corresponds to a $2A_g \rightarrow 1A_g$ transition in which olefinic CH vibrations fail to function as either promoting or accepting modes. Other possibilities, such as aborted photochemical pathways involving new CC bond formation, come to mind. Analogy with unsubstituted 1,3,5-hexatriene (H) may be instructive. Irradiation of *cis*-H at 20 K in an argon matrix gives a thermally unstable product (IR) that was tentatively identified as *exo*-2-vinylbicyclo[1.1.0]butane.[52] The absence of such a product on irradiation of *trans*-H under the same conditions was rationalized on the basis of the expectation that the analogous process in the lowest excited singlet state of *trans*-H would have to give the sterically congested endo isomer.[52] Theoretical calculations favor 1,3-bond formation in the $2A_g$ states of polyenes at the conical intersection (CI) geometry for ultrafast radiationless decay to the ground state,[53,54] and it has been argued, on both theoretical[53,54] and experimental grounds,[55] that such structures play a role in cis−trans photoisomerization (the Hula-Twist mechanism[56]). The possible involvement of cyclopropylmethylene intermediates in the photoisomerization of 1,3-butadienes was proposed by one of us long ago as an alternative to allylmethylene intermediates.[57] Their presence was considered earlier by Srinivasan to account for the formation of cyclopropenes and the related butadiene photodimer.[58] The small calculated torsion angle at the CI for 1,3-butadiene has been thought[54] to explain the supposed low isomerization efficiencies of the 1,3-pentadienes (the 0.1 values cited[57a,59] are for 254 nm excitation which is selectively absorbed by s-cis conformers;[60] excitation of *s-trans,trans*-1,3-pentadiene at 229 nm results in an even lower trans-cis photoisomerization quantum yield[59] of 0.025). This explanation, however, does not account for the highly efficient photoisomerization of the 2,4-hexadienes[57a] and for the regioselective cis → trans photoisomerization of the C_1C_2 bond of *trans*-1,3-pentadiene, revealed by Squillacote's study of 1-*cis*-deuterio-*trans*-1,3-pentadiene.[60] Squillacote proposed

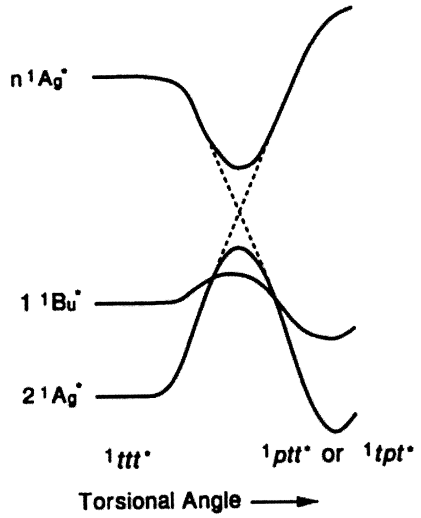

Figure 4. Possible torsional relaxation pathways leading to ^{1}*ttt*-DPH* photoisomerization (schematic, not to scale).

an allyl cation-methylene anion intermediate, analogous to our ptt intermediate, to account for the regioselectivity[60] (zwitterionic 1,3-diene excited-state intermediates were first proposed by Dauben[61]). The very low trans → cis photoisomerization yield of *trans*-H in solution (0.016)[62] is consistent with theoretical computations[53c] which predict that, following S_2 (B_u) → S_1 (A_g) decay in the fs time scale, $S_1 \rightarrow S_0$ radiationless decay occurs very fast to the original ground state via a barrierless process involving a "nontotally symmetric deformation of the molecular backbone" that provides access to a CI.[53c] Such decay is predicted to be slow in *trans,trans*-1,3,5,7-octatetraene because the analogous transition state is calculated to be less accessible energetically.[53c] Two recent studies of internal conversion in all-*trans*-β-carotene may be relevant. The effect of ^{13}C-substitution on the rate of radiationless decay of all-*trans*-β-carotene was found to be significantly larger than that of *d*-substitution leading to the conclusion that the in-phase C═C normal stretching mode plays a major role in the $2A_g \rightarrow 1A_g$ internal conversion.[63] Similarly, a recent CARS spectroscopic study of the population dynamics in vibrational modes that accompany the $S_1 \rightarrow S_0$ radiationless decay of all-*trans*-β-carotene bolsters the conclusion that nuclear motions of CC bonds along the polyene backbone are good candidates for the bottleneck of population flow.[64]

Conclusions

Photoisomerization in the singlet excited state of *ttt*-DPH occurs by competing torsional relaxation pathways involving the terminal and central bonds of the triene moiety leading to twisted intermediates, ^{1}ptt* and ^{1}tpt*, with perpendicular geometries.[11,12] These two processes are differentially enhanced on increasing solvent polarity (MCH to AN). Terminal bond isomerization is enhanced more than 20-fold, whereas central bond isomerization is enhanced only 3-fold.[12] The solvent effect and substituent effects[11] are consistent with the proposal that ^{1}ptt* and ^{1}tpt* are zwitterionic and biradicaloid, respectively, at least in polar solvents.[11] Because these isomerization pathways are subject to large torsional barriers that far exceed ΔE_{BA}, both of these states and higher energy states are viable intermediates for the photoisomerization. Two possible pathways, one for each of the lowest two excited states, are shown in Figure 4, and one may apply preferentially to the central bond and the other to the terminal bonds. The involvement of the higher A_g state is consistent with the modification of the OS mechanism

proposed by Hohlneicher and Dick,[65] and the small torsional barrier in the $1B_u$ state is the pathway favored by Troe and Weitzel for stilbene photoisomerization.[66] Other possibilities can be envisioned.

Terminal bond twisting is sensitive to *d*-substitution, $k_{1H}/k_{1D} = 1.37$ for both olefinic positions, consistent with analogous observations on *trans*-stilbene,[37−43] and with theoretical expectations.[36,44,47] Whether the central bond is similarly sensitive to *d*-substitution remains to be established. The relatively low Arrhenius frequency factor A_{tpt} associated with crossing the torsional barrier for the central bond suggests that the process may be diabatic as in a variant of the OS mechanism for stilbene (e.g., a partially avoided crossing between the $1B_u$ state and a higher nA_g state, $n > 2$).[9] The polar solvent AN enhances the Arrhenius frequency factor A_{ptt} for the terminal bonds to the point where the possibility that this process has been rendered adiabatic must be entertained.

In view of the tendency in vogue to explain the radiationless deactivation of polyenes by invoking ultrafast crossing of CIs, perhaps the most unexpected conclusion is that decay from ^{1}*ttt*-DPH* is dominated by eq 4, an essentially barrierless radiationless pathway, which is insensitive to *d*-substitution at one or both terminal bonds of the triene moiety. Nuclear motions of CC bonds along the triene backbone may be involved in this process as is proposed for polyenes generally[53,54] and as has been found recently for what may be the analogous transition in all-trans-β-carotene.[63,64] However, branching between photoisomers and the original ground state is supposed to occur in the ground state after internal conversion through a CI.[53,54] Such a model clearly does not apply to DPH. The major radiationless decay process is completely divorced from trans → cis photoisomerization, is barrierless within experimental uncertainty, shows no DIE, and occurs in the ns time scale. If ultrafast decay characterizes crossing a CI, then a CI is not involved here. For a CI via partial 1,3-bond formation, or CC bonding on the path to a bicyclobutane to play a role in eq 4, it would have to be neither ultrafast nor along cis−trans photoisomerization reaction coordinates. More work is required to elucidate the mechanism of this highly effective radiationless decay channel.

Acknowledgment. The National Science Foundation, most recently by Grant CHE 9985895, supported this research.

References and Notes

(1) Hudson, B. S.; Kohler, B. E. *Annu. Rev. Phys. Chem.* **1974**, *25*, 437−460.

(2) Hudson, B. S.; Kohler, B. E.; Schulten, K. In *Excited States*; Lim, E. C., Ed.; Academic Press: New York, 1982; Vol. 6, pp 1−95.

(3) Saltiel, J.; Sun, Y.-P. In *Photochromism, Molecules and Systems*; Dürr, H., Bouas-Laurent, H., Eds.; Elsevier: Amsterdam, 1990; pp 64−164.

(4) (a) Pfeiffer, M.; Werncke, W.; Hogiu, S.; Kummrow, A.; Lau, A. *Chem. Phys. Lett.* **1998**, *295*, 56−62. (b) Hogiu, S.; Werncke, W.; Pfeiffer, M.; Lau, A. *Chem. Phys. Lett.* **1999**, *303*, 218−222. (c) Werncke, W.; Hogiu, S.; Pfeiffer, M.; Lau, A.; Kummrow, A. *J. Phys. Chem. A* **2000**, *104*, 4211−4217.

(5) Hilinski, E. F.; McGowan, W. M.; Sears, D. F., Jr.; Saltiel, J. *J. Phys. Chem.* **1996**, *100*, 3308−3311.

(6) Yee, W. A.; O'Neil, R. H.; Lewis, J. W.; Zhang, J. Z.; Kliger, D. S. *Chem. Phys. Lett.* **1997**, *276*, 430−434.

(7) Hogiu, S.; Werncke, W.; Pfeiffer, M.; Lau, A.; Steinke, T. *Chem. Phys. Lett.* **1998**, *287*, 8−16.

(8) Itoh, T.; Kohler, B. E. *J. Phys. Chem.* **1987**, *91*, 1760−1764.

(9) Orlandi, G.; Siebrand, W. *Chem. Phys. Lett.* **1974**, *30*, 352−354.

(10) Birks, J. B.; Birch, D. J. S. *Chem. Phys. Lett.* **1975**, *31*, 608−610. (b) Birks, J. B.; Tripathy, G. N. R.; Lumb, M. D. *Chem. Phys.* **1978**, *33*, 185−194. (c) Birks, J. B. *Chem. Phys. Lett.* **1978**, *54*, 430−434.

(11) Saltiel, J.; Ko, D.-H.; Fleming, A. S. *J. Am. Chem. Soc.* **1994**, *116*, 4099−5000.

(12) Saltiel, J.; Wang, S.; Watkins, L. P.; Ko, D.-H. *J. Phys. Chem. A* **2000**, *104*, 11443−11450.

(13) Cehelnik, E. D.; Cundall, R. B.; Lockwood, J. R.; Palmer, T. J. *J. Phys. Chem.* **1975**, *79*, 1369−1380.

(14) (a) Schael, F. W. *Dissertation*; Technische Universität: Carlo-Wilhelmina zu Braunschweig, Germany, 1995. (b) Schael, F.; Löhmannsröben, H.-G. *Chem. Phys.* **1996**, *206*, 193−210.

(15) Saltiel, J.; Wang, S.; Ko, D.-H.; Gormin, D. A. *J. Phys. Chem. A* **1998**, *102*, 5383−5392.

(16) Nüchter, U.; Zimmermann, G.; Francke, V.; Hopf, H. *Liebigs Ann. Recl.* **1997**, 1505−1515.

(17) Saltiel, J.; Crowder, J. M.; Wang, S. *J. Am. Chem. Soc.* **1999**, *121*, 895−902.

(18) Vollhardt, K. P. C.; Winn, L. S. *Tetrahedron Lett.* **1985**, *26*, 709−12.

(19) Moses, F. G.; Liu, R. S. H.; Monroe, B. M. *Mol. Photochem.* **1969**, *1*, 245−249.

(20) Hammond, H. A.; DeMeyer, D. E.; Williams, J. L. R. *J. Am. Chem. Soc.* **1969**, *91*, 5180−5181.

(21) Valentine, D., Jr.; Hammond, G. S. *J. Am. Chem. Soc.* **1972**, *94*, 3449−3454.

(22) Saltiel, J.; Sears, D. F., Jr.; Ko, D.-H.; Park, K. M. In *Handbook of Organic Photochemistry*; Horspool, W. M., Song, P.-O., Eds.; CRC Press: London, 1995; Section 1, pp 3−15.

(23) Melhuish, W. H. *J. Phys. Chem.* **1961**, *65*, 229−235.

(24) Meech, S. R.; Phillips, D. *J. Photochem.* **1983**, *23*, 193−217.

(25) Saltiel, J.; Charlton, J. L. In *Rearrangements in Ground and Excited States*; de Mayo, P., Ed.; 1980; Vol. III, pp 25−89.

(26) (a) Ko, D.-H. Ph.D. Dissertation, Florida State University, Tallahassee, FL, 1997. (b) Wang, S. Ph.D. Dissertation, Florida State University, Tallahassee, FL, 1998.

(27) (a) Robinson, G. W.; Frosch, R. P. *J. Chem. Phys.* **1962**, *37*, 1962. (b) Robinson, G. W.; Frosch, R. P. *J. Chem. Phys.* **1963**, *38*, 1187.

(28) Lower, S. K.; El-Sayed, M. A. *Chem. Rev.* **1966**, *66*, 199.

(29) Jortner, J.; Rice, S. A.; Hochstrasser, R. M. *Adv. Photochem.* **1969**, *7*, 149−309.

(30) Siebrand, W. *The Triplet State*; Beirut Symposium, 1967; Zahlan, A. B., Ed.: Cambridge University Press: Cambridge, 1967; p 31.

(31) Hirota, N.; Hutchison, C. A., Jr. *J. Chem. Phys.* **1967**, *46*, 1561.

(32) (a) Martin, T. E.; Kalantar, A. H. *J. Chem. Phys.* **1968**, *48*, 4996. (b) Martin, T. E.; Kalantar, A. H. *Chem. Phys. Lett.* **1968**, *1*, 623.

(33) (a) Watts, R. J.; Strickler, S. J. *J. Chem. Phys.* **1968**, *49*, 3967. (b) Burke, T. D.; Watts, R. J.; Strickler, S. J. *J. Chem. Phys.* **1969**, *50*, 5425.

(34) Simpson, J. D.; Offen, H. W.; Burr, J. D. *Chem. Phys. Lett.* **1969**, *2*, 383.

(35) Henry, B. R.; Charlton, J. L. *J. Am. Chem. Soc.* **1973**, *95*, 2782−2785.

(36) Henry, B. R.; Siebrand, W. *J. Chem. Phys.* **1971**, *54*, 1072. (b) Henry, B. R.; Siebrand, W. *Chem. Phys. Lett.* **1969**, *3*, 327.

(37) Saltiel, J.; D'Agostino, J. T.; Herkstroeter, W. G.; Saint-Ruf, G.; Buu-Hoï, N. P. *J. Am. Chem. Soc.* **1973**, *95*, 2543−2549.

(38) Caldwell, R. A. *Pure Appl. Chem.* **1984**, *56*, 1167−1177.

(39) Heinrich, G.; Holzer, G.; Blume, H.; Schulte-Frohlinde, D. *Z. Naturforsch. B* **1970**, *25*, 496.

(40) Courtney, S. H.; Balk, M. W.; Phillips, L. A.; Web, S. P.; Yang, D.; Levy, D. H.; Fleming, G. R. *J. Chem. Phys.* **1988**, *89*, 6697.

(41) Saltiel, J.; Waller, A. S.; Sears, D. F., Jr.; Garrett, C. Z. *J. Phys. Chem.* **1993**, *97*, 2515−2522.

(42) The corresponding effects on the transmission coefficients are small (10−15%), but the changes are in opposite directions in the two solvents.[30]

(43) Felker, P. M.; Zewail, A. H. *J. Phys. Chem.* **1985**, *89*, 5402−5411.

(44) Negri, F.; Orlandi, G. *J. Phys. Chem.* **1991**, *95*, 748−757 and references cited.

(45) Saltiel, J.; Waller, A. S.; Sears, D. F., Jr. *J. Am. Chem. Soc.* **1993**, *115*, 2453−2464.

(46) Caldwell, R. A.; Misawa, H.; Healy, E. F.; Dewar, M. J. S. *J. Am. Chem. Soc.* **1987**, *109*, 6869−6870.

(47) Olson, L. P.; Niwayama, S.; Yoo, H.-Y.; Houk, K. N.; Harris, N. J.; Gajewski, J. J. *J. Am. Chem. Soc.* **1996**, *118*, 886−892.

(48) Brouwer, A. M.; Cornelisse, J.; Jacobs, H. J. C. *J. Photochem. Photobiol. A: Chem.* **1988**, *42*, 313−320.

(49) Saltiel, J. *J. Am. Chem. Soc.* **1968**, *90*, 6394−6400.

(50) Saltiel, J.; Sears, D. F., Jr.; Sun, Y.-P.; Choi, J.-O. *J. Am. Chem. Soc.* **1992**, *114*, 3607−3612.

(51) (a) Siebrand, W. *J. Chem. Phys.* **1967**, *46*, 440; *47*, 2411. (b) Klessinger, M.; Michl, J. *Excited States and Photochemistry of Organic Molecules*; VCH Publisher: New York, 1995; p 254.

(52) Datta, P.; Goldfarb, T. D.; Boikess, R. S. *J. Am. Chem. Soc.* **1971**, *93*, 5189−5193.

(53) (a) Olivucci, M.; Bernardi, F.; Celani, P.; Ragazos, I. N.; Robb, M. A. *J. Am. Chem. Soc.* **1994**, *116*, 1077−1085. (b) Celani, P.; Garavelli, M.; Ottani, S.; Bernardi, F.; Robb, M. A.; Olivucci, M. *J. Am. Chem. Soc.*

1995, *117*, 11584−11585. (c) Garavelli, M.; Celani, P.; Bernardi, F.; Robb, M. A.; Olivucci, M. *J. Am. Chem. Soc.* **1997**, *119*, 11487−11494.

(54) For a recent review of polyene photophysics, see: Fuss, W.; Haas, Y.; Zilberg, S. *Chem. Phys*. **2000**, *259*, 273−295.

(55) Müller, A. M.; Lochbrunner, S.; Schmid, W. E.; Füss, W. *Angew. Chem., Int. Ed*. **1998**, *37*, 505−507.

(56) (a) Liu, R. S. H.; Asato, A. E. *Proc. Natl. Acad. Sci. U.S.A.* **1985**, *82*, 259−263. (b) Liu, R. S. H.; Hammond, G. S. *Proc. Natl. Acad. Sci. U.S.A.* **2000**, *97*, 11153−11158. (c) Liu, R. S. H. *Acc. Chem. Res.* **2001**, *34*, 555−562.

(57) (a) Saltiel, J.; Metts, L.; Wrighton, M. *J. Am. Chem. Soc.* **1970**, *92*, 3227−3229. (b) Saltiel, J.; D′Agostino, J. T.; Megarity, E. D.; Metts, L.; Neuberger, K. R.; Wrighton, M.; Zafiriou, O. C. *Org. Photochem.* **1973**, *3*, 1−113.

(58) Srinivasan, R. *J. Am. Chem. Soc.* **1968**, *90*, 4498−4499.

(59) Vanderlinden, P.; Boué, S. *J. Chem. Soc. Chem. Commun.* **1975**, 932−933.

(60) Squillacote, M. E.; Semple, T. C. *J. Am. Chem. Soc*. **1987**, *109*, 892−894.

(61) (a) Dauben, W. G.; Ritscher, J. S. *J. Am. Chem. Soc*. **1970**, *92*, 2925−2926.

(62) (a) Jacobs, H. J. C.; Havinga, E. *Adv. Photochem*. **1979**, *11*, 305. (b) Vroegop, P. J.; Lugtenburg, J.; Havinga, E. *Tetrahedron* **1973**, *29*, 1393.

(63) Nagae, H.; Kuki, M.; Zhang, J.-P.; Sashima, T.; Mukai, Y.; Koyama, Y. *J. Phys. Chem. A* **2000**, *104*, 4155−4166.

(64) Siebert, T.; Schmitt, M.; Engel, V.; Materny, A.; Kiefer, W. *J. Am. Chem. Soc.* **2002**, *124*, 6242−6243.

(65) Hohlneicher, G.; Dick, B. *J. Photochem.* **1984**, *27*, 215.

(66) Troe, J.; Weitzel, K.-M. *J. Chem. Phys.* **1988**, *88*, 7030.